Methods, Results, and Discussion: Code Validation for SWIRL

Jeffrey Severino
University of Toledo
Toledo, OH 43606
email: jseveri@rockets.utoledo.edu

May 6, 2022

0.1 Methods

A comparison was conducted for a hollow cylinder undergoing uniform flow with acoustic liners along the outer duct perimeter. The azimuthal mode number, reduced frequency, mach number and duct liner admittance is reported below,

$$\begin{aligned} m &= 2 \\ k &= \frac{\omega r_T}{A_T} = -1 \\ M_x &= 0.5 \\ \eta_T &= 0.72 + 0.42i \end{aligned}$$

1 Results

Figure 1 shows the effect of varying grid points on the dimensionless axial wavenumbers for four different grids using a second order differencing scheme to obtain the radial derivatives in the LEE. When compared to the thirty-two point grid , the one hundred twenty eight point gird shows axial wave numbers that are more parallel to the imaginary axis. However, the wavenumbers show consistent agreement for the convective wavenumbers across all four grids. into their categories as opposed to being sporadic. The imaginary component of the wavenumbers change the most with varying grid points.

Once the axial wavenumbers are computed, they are sorted according to the number of times that the associated radial pressure mode crosses zero. This is done by computing the phase of each mode ϕ , where $\phi = \arctan \frac{Imp_{i=1}}{Rep_{i=1}}$, and then multiplying the $i = 2$ through $i = n$ points by $\exp -i\phi$. The index n is the last grid point. By doing this, the phase of each mode was shifted such that it was in agreement with the phase of the pressure mode at the first grid point. After this was completed, then the zero crossings were found by identifying a sign change in the mode. The modes that were reported in Kousen's Table 4.3 are shown in Figures 2-19. Figures 2-10 show the propagating (cut-on) modes and Figures 11-19 show the decaying modes (cut-off).

1.1 Propagating (Cut-on) pressure modes

2 Issues and Concerns

3 Planned Research

- Compute the L2 of ϕ from grid to grid.
- Clean up axial wavenumber plots so that varying grids are easier to see.
- Report the findings from the fourth order study
- Complete the results section draft (add better captions)
- Discuss Results

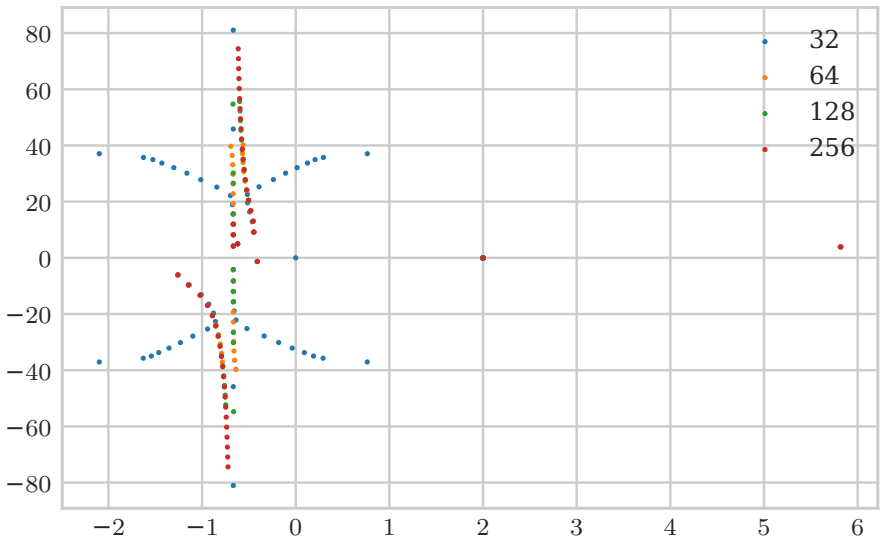

Figure 1: The Dimensionless Axial Wavenumbers that Represent the Discrete Acoustic Disturbances obtained in Table 4.3 in [Kousens] - Cylinder, Uniform Mean Flow with Liner.

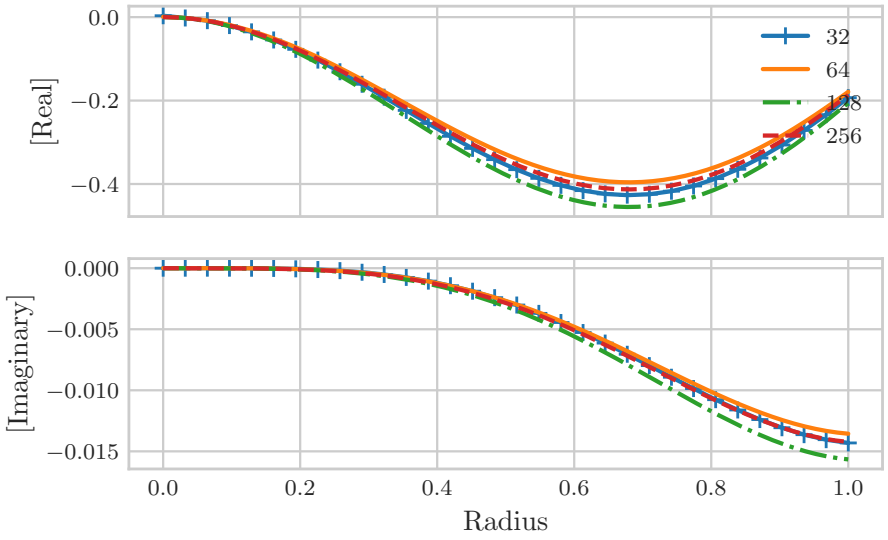

Figure 2: Propagating Mode $\gamma_0^+ = 0.620 - 5.014i$

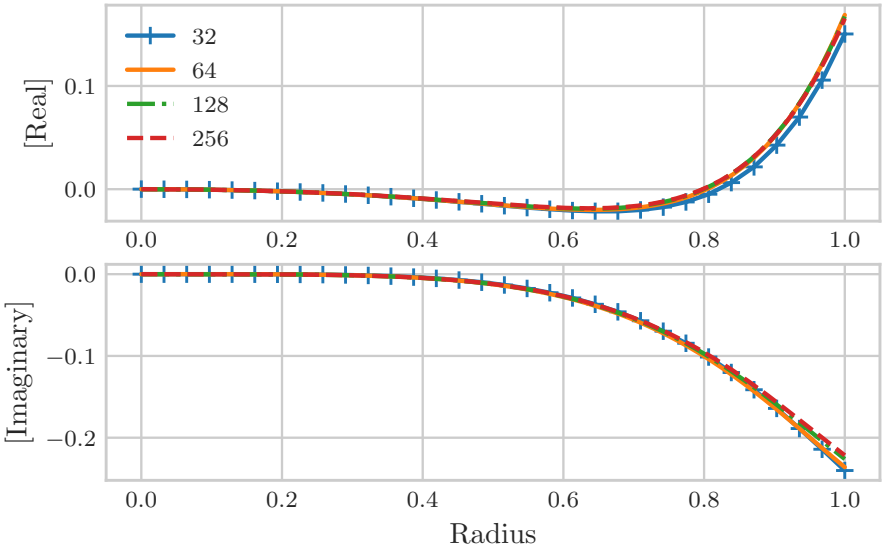

Figure 3: Propagating Mode $\gamma_1^+ = -5.820 - 3.897i$

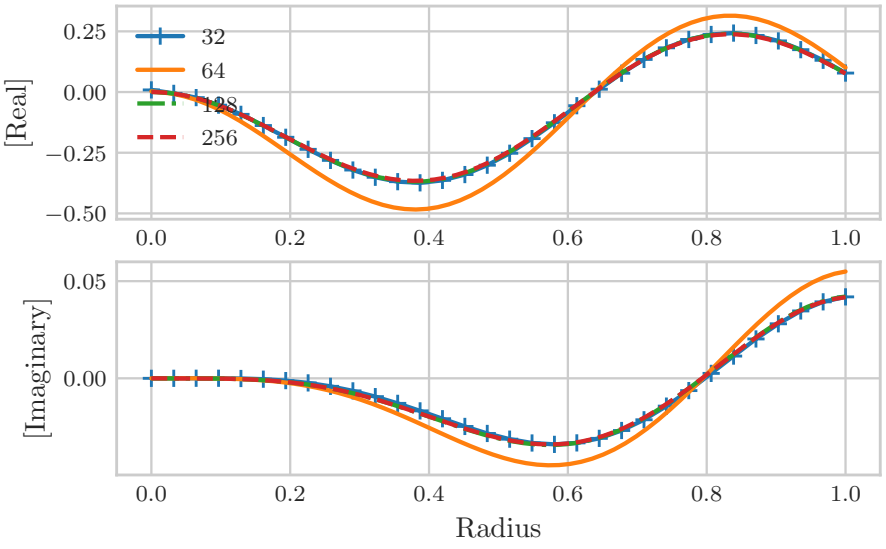

Figure 4: Propagating Mode $\gamma_2^+ = 0.445 - 9.187i$

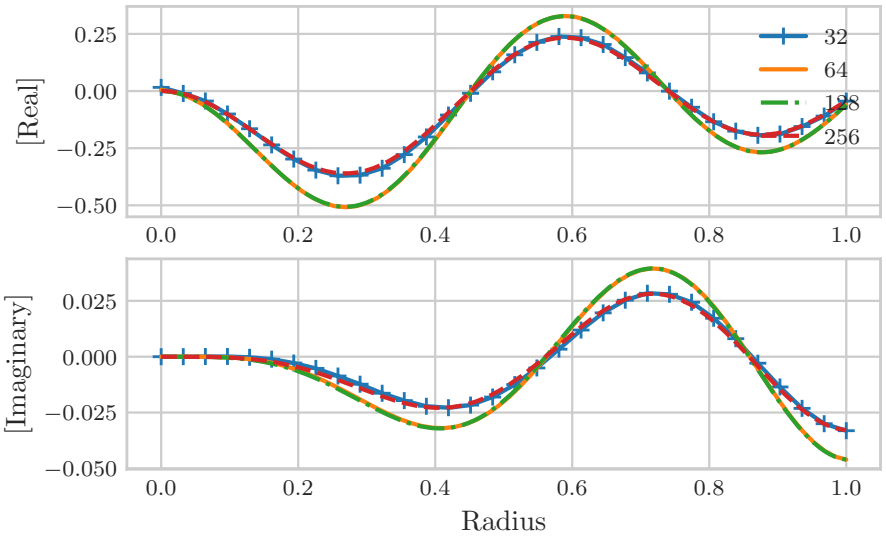

Figure 5: Propagating Mode $\gamma_3^+ = 0.453 - 13.062i$

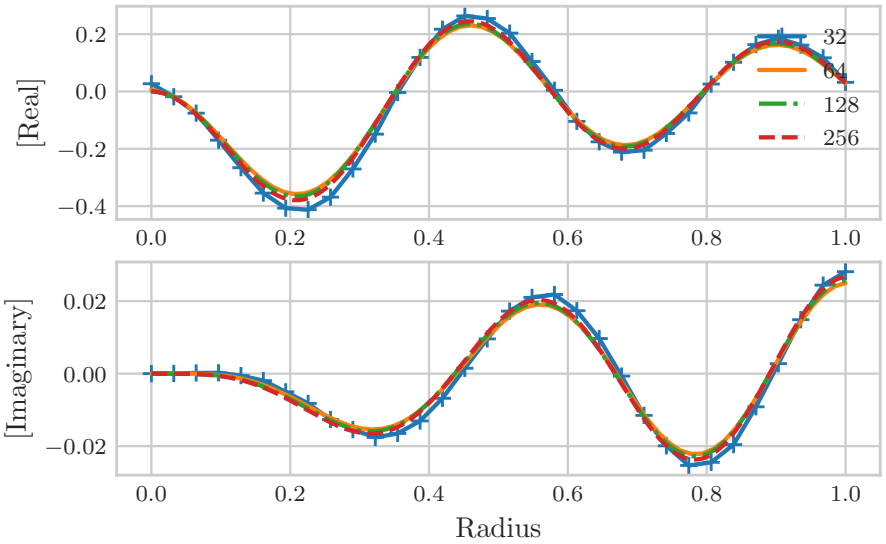

Figure 6: Propagating Mode $\gamma_4^+ = 0.480 - 16.822i$

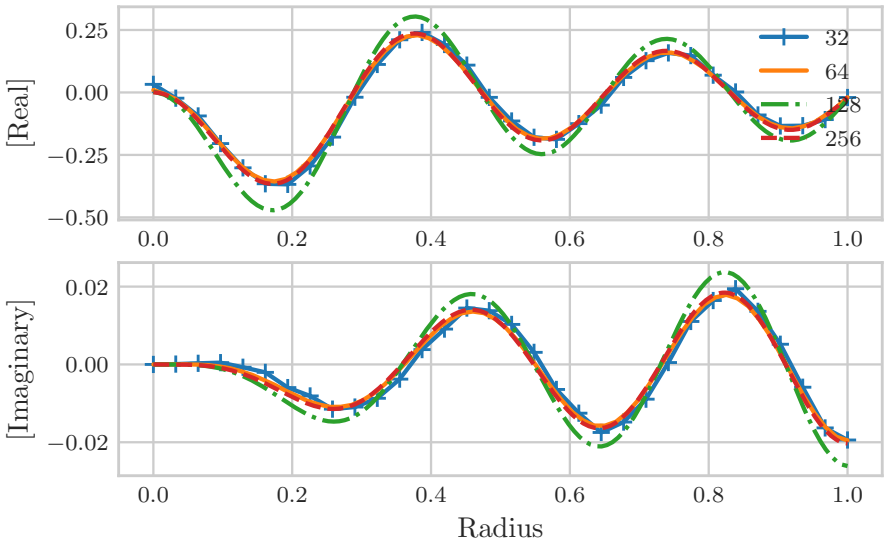

Figure 7: Propagating Mode $\gamma_5^+ = 0.503 - 20.531$

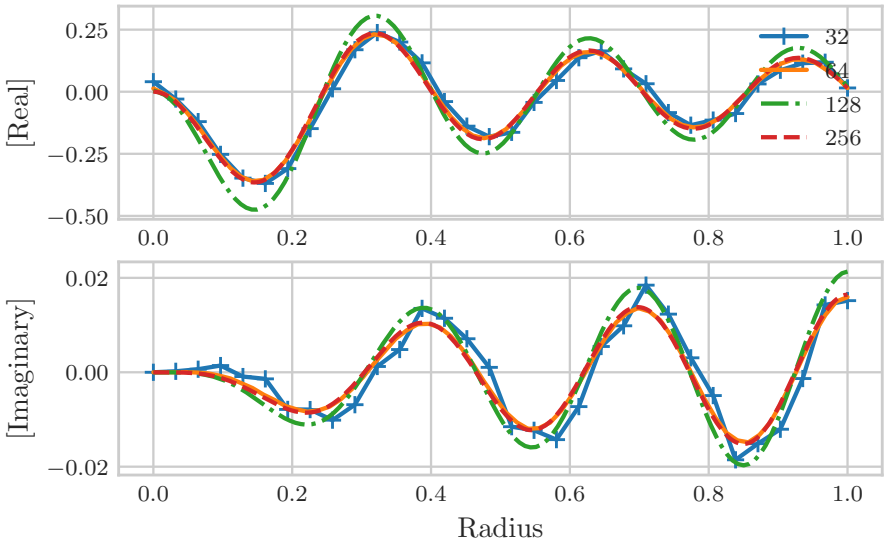

Figure 8: Propagating Mode $\gamma_6^+ = 0.522 - 24.213i$

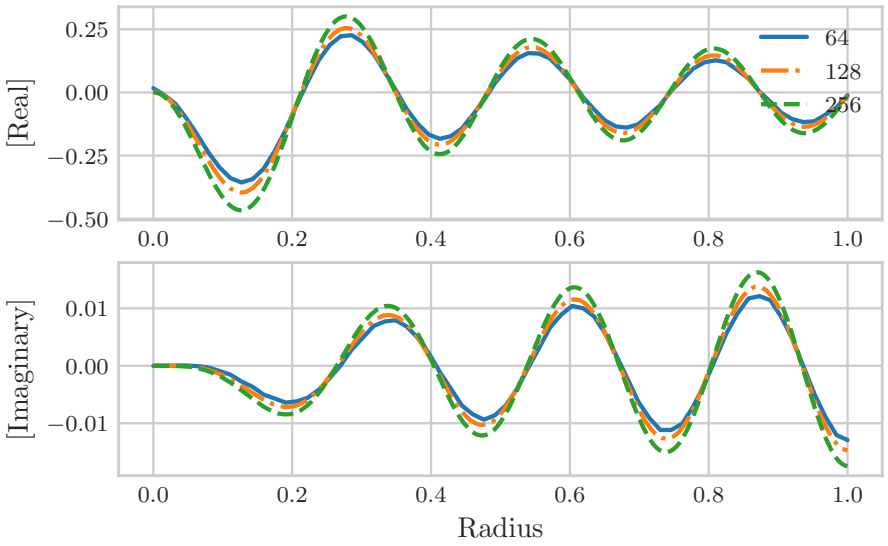

Figure 9: Propagating Mode $\gamma_7^+ = 0.538 - 27.880i$

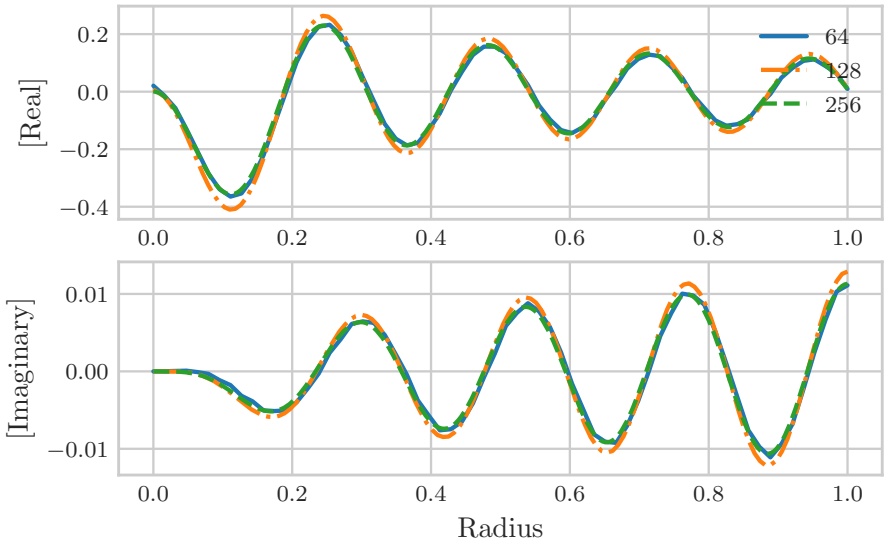

Figure 10: Propagating Mode $\gamma_8^+ = 0.550 - 31.537$

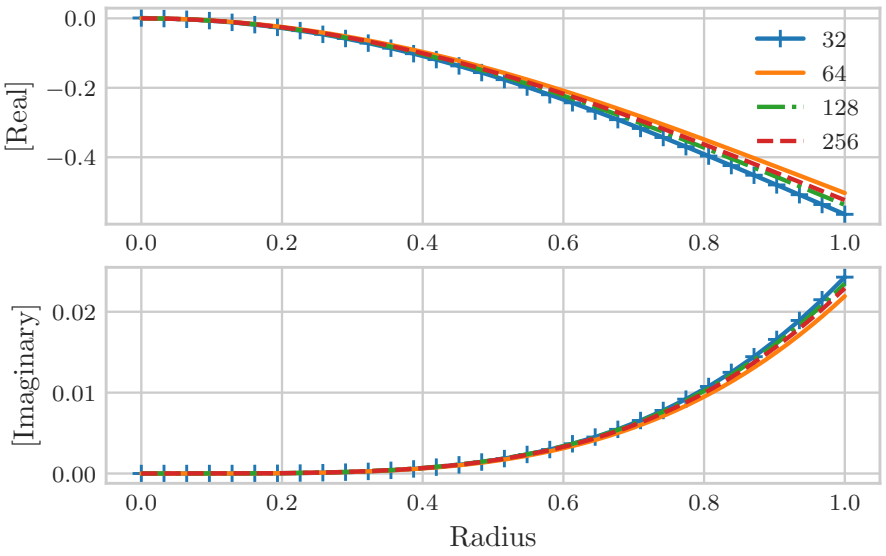

Figure 11: Propagating Mode $\gamma_0^- = 0.410 + 1.290i$

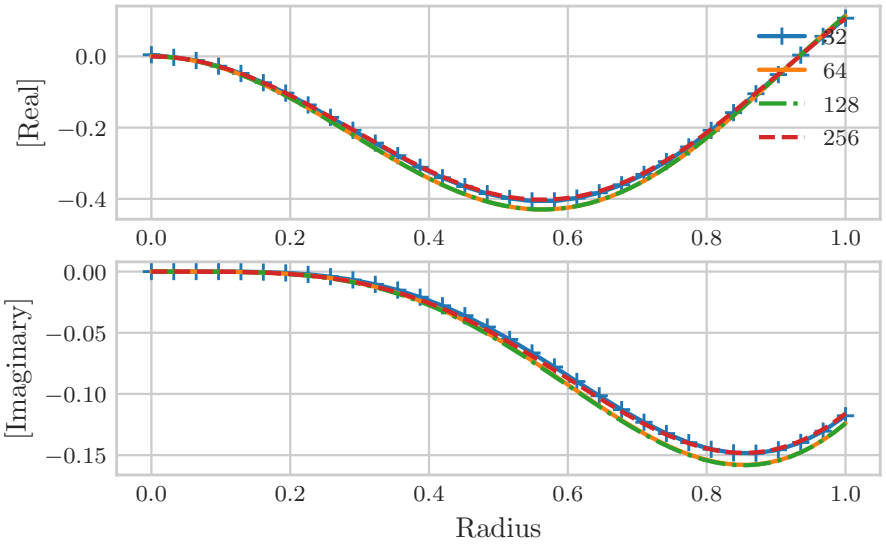

Figure 12: Propagating Mode $\gamma_1^- = 1.259 + 6.085i$

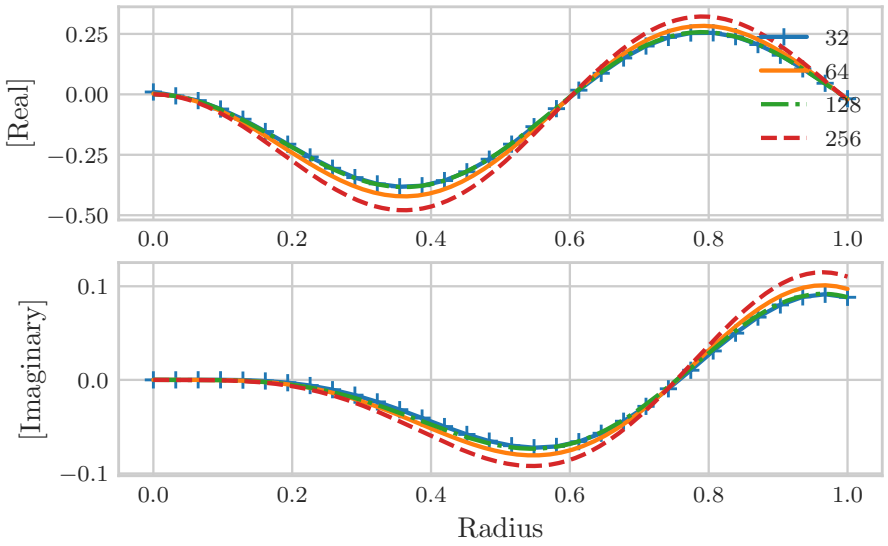

Figure 13: Propagating Mode $\gamma_2^- = 1.146 + 9.668i$

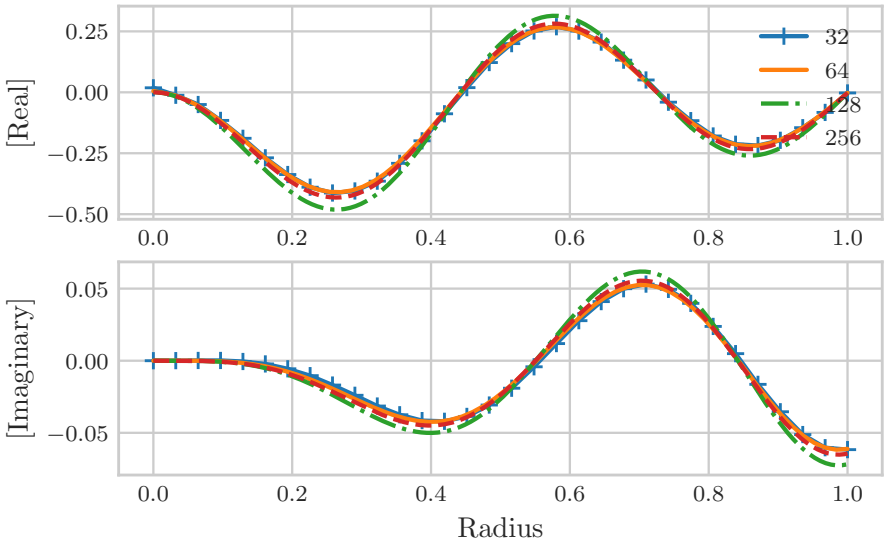

Figure 14: Propagating Mode $\gamma_3^- = 1.022 + 13.315i$

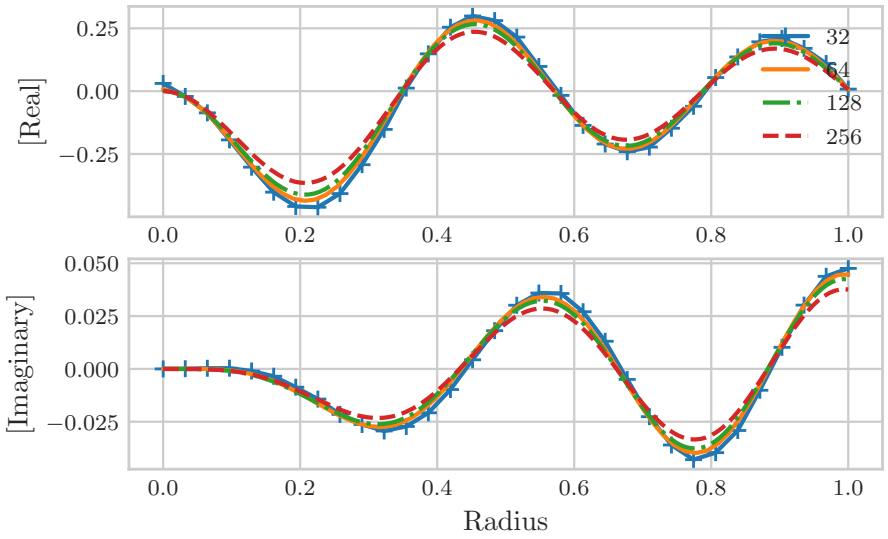

Figure 15: Propagating Mode $\gamma_4^- = 0.943 + 16.977i$

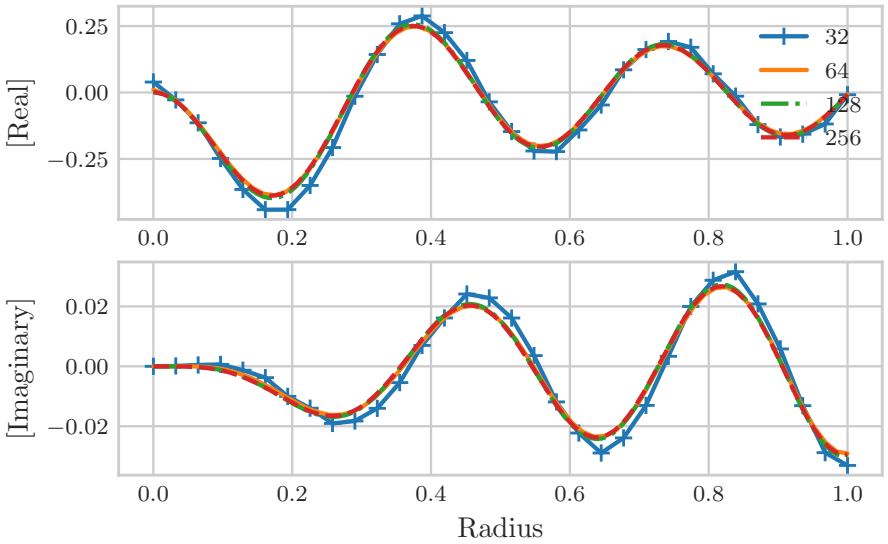

Figure 16: Propagating Mode $\gamma_5^- = 0.891 + 20.635i$

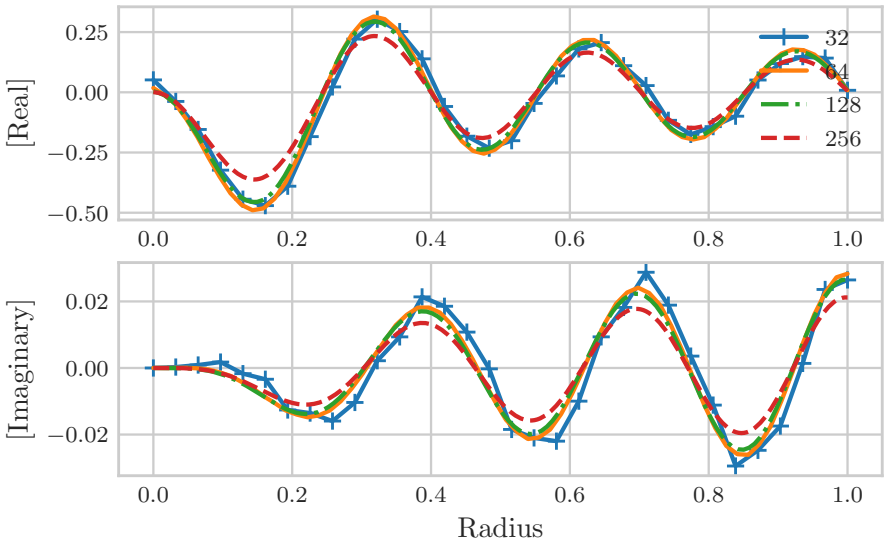

Figure 17: Propagating Mode $\gamma_6^- = 0.855 + 24.288i$

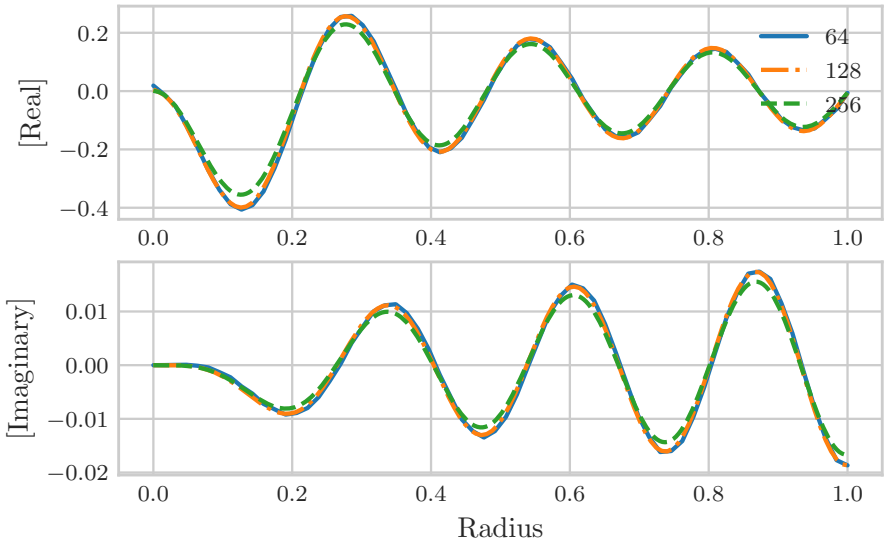

Figure 18: Propagating Mode $\gamma_7^- = 0.829 + 27.937i$

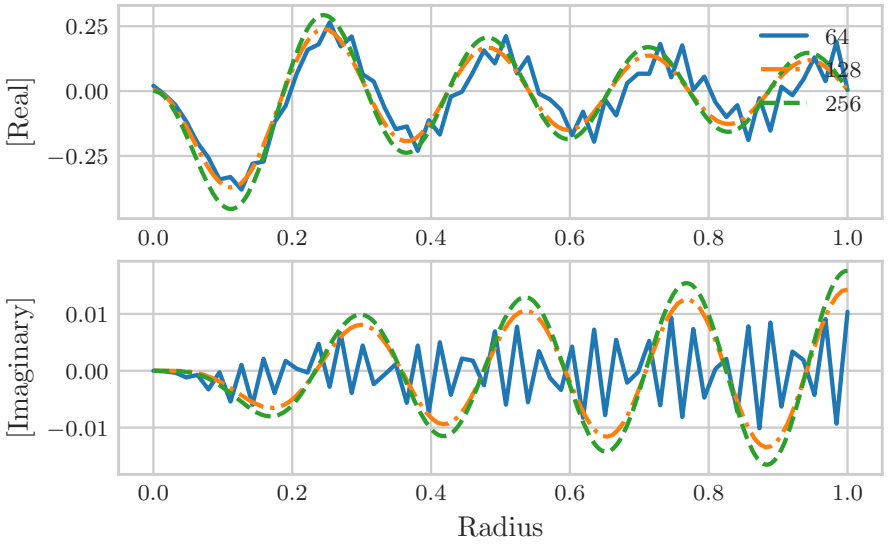

Figure 19: Propagating Mode $\gamma_8^- = 0.809 + 31.581i$